Lab on a Chip

An array microhabitat device with dual gradients revealed synergistic roles of nitrogen and phosphorous on the growth of microalgae

Journal:	*Lab on a Chip*
Manuscript ID	LC-ART-11-2019-001153.R1
Article Type:	Paper
Date Submitted by the Author:	08-Jan-2020
Complete List of Authors:	Liu, Fangchen; Cornell University, Biological and Environmental Engineering Yazdani, Mohammad; Cornell University, Biological and Environmental Engineering Ahner, Beth; Cornell University, Biological and Environmental Engineering Wu, Mingming; Cornell University, Biological and Environmental Engineering

ARTICLE

An array microhabitat device with dual gradients revealed synergistic roles of nitrogen and phosphorous in the growth of microalgae

Received 00th January 20xx,
Accepted 00th January 20xx

DOI: 10.1039/x0xx00000x

Fangchen Liu, Mohammad Yazdani, Beth A. Ahner and Mingming Wu*

Harmful Algal Blooms (HABs) are an emerging environmental problem contaminating water resources and disrupting the balance of the ecosystems. HABs are caused by the sudden growth of photosynthetic algal cells in both fresh and marine water, and have been expanding in extent and appearing more frequently due to the climate change and population growth. Despite the urgency of the problem, the exact environmental conditions that trigger HABs are unknown. This is in part due to the lack of high throughput tools for screening environmental parameters in promoting the growth of photosynthetic microorganisms. In this article, we developed an array microhabitat device with well defined dual nutrient gradients suitable for quantitative studies of multiple environmental parameters in microalgal cell growth. This device enabled an ability to provide 64 different nutrient conditions [nitrogen (N), phosphorous (P), and N:P ratio] at the same time, and the gradient generation took less than 90 min, advancing the current pond and test tube assays in terms of time and cost. Using a photosynthetic algal cell line, *Chlamydomonas reinhardtii*, preconditioned in co-limited media, we revealed that N and P synergistically promoted cell growth. Interestingly, no discernible response was observed when single P or N gradient was imposed. Our work demonstrated the enabling capability of the microfluidic platform for screening effects of multiple environmental factors in photosynthetic cell growth, and highlighted the importance of the synergistic roles of environmental factors in algal cell growth.

Introduction

Harmful Algal blooms (HABs) are characterized by a sudden growth of microalgae or cyanobacteria that disrupts the life forms in the affected aquatic ecosystem and degrades water quality for human use[1-3]. Driven by accelerated eutrophication, the occurrence of HABs is persistent and intensifying globally, such as in Lake Erie of the Great Lakes, costal area in southern Chile, Baltic sea in Europe, and Lake Taihu in China[4-9]. The bloom species can produce toxins including heptatoxins, neurotoxins and dermatotoxins threatening human health[10-12]. The onset of HABs are known to be caused by multiple environmental factors including nutrients, temperature and light intensity. Currently, there is no effective method to predict, disrupt and prevent HABs. Traditionally, HABs were managed by controlling phosphorous (P), only recently, the paradigm has shifted to include the management of nitrogen (N) in addition to P [5, 13, 14]. We also know that temperature, light, and fluid flows can modulate the onset of HABs [7, 15]. Despite the urgency of the problem, a systematic understanding of the roles of multiple environmental factors in the outbreak of HABs, in particular at the cellular level, is largely unexplored. This is, in part, due to the lack of high throughput tools for studies of effects of many environmental factors in algal growth.

A number of approaches have been used to investigate the roles of environmental cues in the onset of HABs. A traditional method is to sample directly from the bloomed lakes or ponds and measure physical factors such as water temperature and clarity/turbidity; chemical factors such as dissolved oxygen, nutrients, and pH; and biological factors such as algae abundance and bacteria community [16, 17]. This approach is useful in monitoring long-term bloom behaviour in a lake or pond, and provides realistic information on the variation of environmental factors associated with blooms. However, it is difficult to carry out a controlled and mechanistic study in the lake or pond setting. A common approach in the lab is to study cell growth rate using a series of culture flasks or chemostats that are subjected to different environmental conditions. Using this approach, it was found that complex combinations of N and P concentration and their ratio, together with temperature and light intensity, could modulate algal biomass accumulation and/or toxin production[18-20]. However, these experiments often require large amounts of reagents and time, thus difficult in screening a range of values for each environmental factor to achieve a quantitative understanding. In particular, single cell level work is not possible. As a result, systematic studies on the effects of multiple environmental cues remain to be done.

Microfluidics provides a high throughput format for fast screening of multiple environmental factors and allows for real time monitoring of microalgal growth under well controlled

Department of Biological and Environmental Engineering, Cornell University, Ithaca, NY, USA.E-mail: mw272@cornell.edu
Electronic Supplementary Information (ESI) available: [details of any supplementary information available should be included here]. See DOI: 10.1039/x0xx00000x

environmental conditions. Studies of mammalian cells and bacteria under single/dual gradients have been carried out successfully in the past[21-25]. However, studies of photosynthetic microorganism under well defined gradients have been limited to millimetre scales[26, 27], or in mixing channel format where cells are subjected to convective flow [28, 29] or in single gradient[30]. In this article, we present a diffusion based array microhabitat device with stable dual chemical gradients. This device integrates the array microhabitat format together with the dual gradients for providing multiple environmental conditions for photosynthetic cell growth. It is an advancement of our early version of the hydrogel based device where a single gradient was established[30]. The dual gradient device enabled an ability to probe the synergistic effects of two important factors for algal growth, N and P, for the first time in a high throughput platform. Using this device, we studied the synergistic effects of N and P on the growth of a model algal species, *Chlamydomonas reinhardtii (C. reinhardtii)*. We note that this device can be easily extended to include other environmental cues such as temperature and light intensity.

Experimental Methods

Silicon master fabrication

The silicon master was fabricated using a 2-layer photo lithography method with SU-8 negative photoresist. The fabrication was done at the Cornell Nanoscale Science and Technology Facility (CNF) using a similar protocol described previously[30]. Briefly, the two layers, one layer for the 200 µm depth sink and source channels and the other layer for the 100 µm depth microhabitats were patterned separately onto a silicon wafer coated with SU8 and then etched in one last step. First, a layer of 100 µm SU-8 2100 (MicroChem Corp., Westborough, MA) was spun on the silicon wafer (100 mm diameter, 525 ± 20 µm-thick) at 3000 rpm for 30 sec. Then the wafer was soft baked for 10 hours. [Soft bake: (i)10 minutes in room temperature, ramp up to 65 °C at the rate of 2 °C /min, left at 65 °C for an hour; (ii) ramp to 95 °C at 2 °C/min and kept at 95 °C for 8 hours; (iii) The hot plate was turned off after that and let cool down to room temperature by natural convection]. After the resist layer was left on the hot plate overnight to reach thermal and internal tension equilibrium, it was exposed to the pattern of microhabitats and channels using 365nm filter at 250 mJ/cm^2 on a contact aligner (ABM Contact Aligner, ABM Inc., Silicon Valley, CA), followed by leaving it for 30-minute under room temperature. Second, another layer of 100µm thick SU8 layer was spun, relaxed and soft baked. The post exposure bake (PEB) of the first layer of photoresist was combined with the soft bake of the second layer. The exposed regions on the first layer crosslinked and became visible during PEB, which included the alignment makers that were used for the alignment of the second layer. Exposure of the second layer to the pattern of channels was done on the same contact aligner at 320 mJ/ cm^2 followed by relaxation. [PEB: (i) ramp up hot plate temperature from room temperature to 65°C at 2°C/min and keep for 5 minutes; (ii) ramp up temperature to 95°C at the same rate and keep for 15 minutes; (iii) turn off plate and let it stay for 12 hours.] Both layers were then developed using SU-8 developer (MicroChem) and the residual developer was removed using isopropanol and DI water. A 4-hour hard bake was performed at 150°C on the hot plate with the same ramping rate from room temperature, followed by an 8-hour relaxation time. (1H, 1H, 2H, 2H-Perfluorooctyl)Trichlorosilane (FOTS) was then coated on the hard-baked pattern using the molecular vapor deposition system (MVD-100, Applied MicroStructures) to make the surface hydrophobic and non-stick for peeling off of the agarose gel. The height of the features on the wafer was measured using a profilometer (P10 Profilometer, Tencor). Note that slow temperature ramping and relaxation time throughout the fabrication process is critical to minimize internal stress in order to avoid resist detachment.

Microfluidic device assembly and experimental setup

The array microhabitat device pattern was transferred to a 1mm thick agarose membrane using a soft lithography method. First, about 3mL boiled 3% agarose solution in DI water was poured on the silicon master surrounded by a 1mm-thick spacer in a biosafety cabinet. Then the gel was peeled off after it was polymerized in room temperature, and immediately placed in media for at least 2 hours before device assembly. To assemble a device, we first place 200 µL of *C. reinhardtii* (2.7×10^6 cells per mL) cell culture on the patterned agarose surrounded by the spacer, the gel was then sandwiched between a Plexiglas manifold and a 1 inch × 3 inch glass slide. Good seal of the device was ensured by screwing the Plexiglas manifold down to a stainless-steel frame. The initial cell number in each microhabitat was usually 1 to 6 cells. Empty microhabitats due to randomness of the seeding were omitted in data analysis.

To control the flow along the side channels, a syringe pump (KDS230, KD Scientific, Holliston, MA) and two 10 mL syringes (Exelint International Co., Redondo Beach, CA) were used. Media from the syringes were pumped into the microfluidic channels through medical grade tubing (ID = 0.20in, PharMed BPT, Cole-Parmer, Vernon Hills, IL) and gel-loading tips. A flow rate of 1 µL/min was used in the experiments. The experiment was set up by the microscope, where the microfluidic chip was firmly secured on the stage and covered by a paper box to avoid convective flow in the room for humidity control. The illumination for photosynthetic growth was provided by two LED (3700K) panels mounted in the box with same distance to the microfluidics chip. Light intensity was measured to be 12 µmols/(m^2·s) and uniform at the chip locations using a Photosynthetically Active Radiation meter (Apogee MQ-501). The temperature of the microscope room was controlled at 25°C, and the temperature inside the illuminated box was measured to be 25-26°C.

Imaging and data analysis

All images were taken automatically while cells were growing within the microhabitats in the microfluidic device that was placed on the microscope stage. A typical experiment ran about 5-6 days. For most part of the experiments, the cells were exposed to a fixed illumination LED light at 12 µmols/(m^2·s) for

photosynthetic organism. When imaging, the LED light was turned off, and a light source from microscope was used. An epi-fluorescence microscope (Olympus IX81, Center Valley, CA), together with an EMCCD camera (ImagEM X2 EM-CCD camera, Hamamatsu Photonics K.K.) were used in all our experiments. Olympus software cellSense was used to control the positions of the microscope stage (MS-2000, Applied Scientific Instrumentation, Eugene, OR), fluorescence filters and imaging. For fluorescence imaging of *C. reinhardtii* cells, a fluorescent light source (X-Cite 120PC Q, Excelitas Technologies Corp.), a 488/10 nm single bandpass excitation filter (Semrock, Rochester, NY) and a 440/521/607/700 quad-bandpass emission filter (Semrock, Rochester, NY) were used. 10 blank images were taken before each experiment and later averaged in imageJ for background subtraction. Typically, fluorescence images were taken at a 4-hour interval for 5 days total. Bright field images were taken at every 30 minutes for 5 days. Images were post-processed using imageJ (shareware from National Institute of Health). After background image subtraction, cell numbers were computed using the total fluorescence from each habitat. Here, we assume that fluorescence is proportional to the cell number which was validated using the bright field image in our experiments. The specific growth rates were obtained by fitting the exponential growth phase of the growth curve to an exponential function.

Cell culture and media

C. reinhardtii wild type strain CC-125 was obtained from the Stern Laboratory at the Boyce Thompson Institute of Plant Research at Cornell University. Cells were maintained in MM/0.1TAP, which is minimal medium with 10% TAP (Tris Acetate Phosphate) medium (2mM Tris, 1.7mM Acetate, 0.68 mM K_2HPO_4, 0.45mM KH_2PO_4, 7.5 mM NH_4Cl, and other salts including 0.34 mM CaCl2) prepared using an established protocol[31] with trace metal elements concentrations as described in Hutner et al.[32] 5-mL cell culture was maintained in 15mL glass tubes in a temperature-controlled incubator (New Brunswick Innova 44, Eppendorf) under a 12 µmols/(m^2·s) illumination using fluorescent light bulbs (4200K, Lights of America; 3500K, SLI Lighting E-LITE). The maintenance culture was transferred every two weeks.

For nutrient gradient experiments in the microfluidic device, the cells were pre-conditioned in media limited on both nitrogen and phosphorous in advance. We will refer to these cells co-limited cells in the rest of the paper. Co-limit cell protocol: (i) 0.5 mL of a 2-week old culture was transferred into 5 mL of medium with low nitrogen and no phosphorous (750 µM N, 0 P) and kept to grow for 2 weeks; (ii) 0.5 mL of the low N, no P conditioned culture was centrifuged at 1500g for 1.5 minutes and washed using no N, no P medium twice, and then used to inoculate 5 mL of no N, no P culture; (iii) after 2 days, when the cell density was 2.7×10^5 cells per mL, the culture was concentrated by 10-fold and used to seed the microhabitats. The cell density in tube cultures was evaluated using a hemocytometer. The N form used in the nutrient gradient experiments was ammonium, and P form, phosphate (K_2HPO_4 : KH_2PO_4 = 0.68 : 0.45).

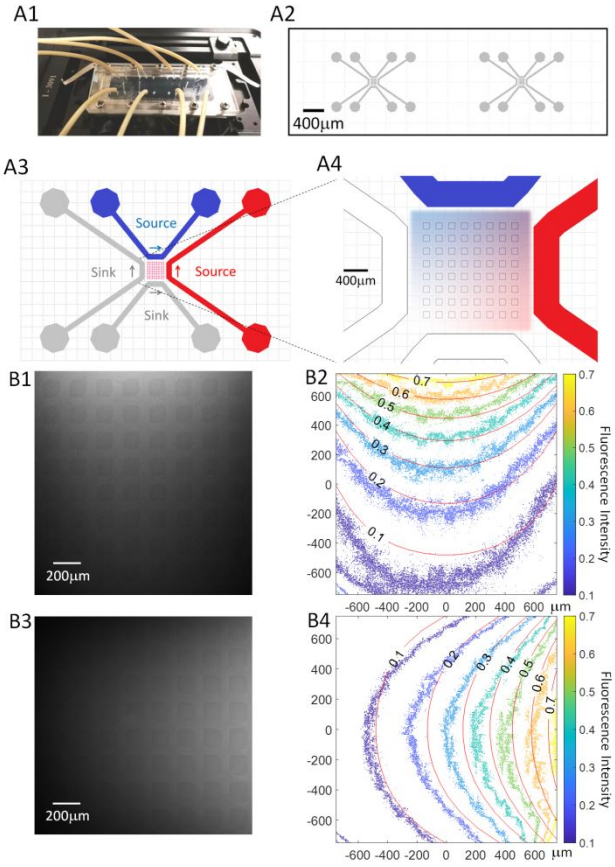

Figure 1. Design and validation of the microfluidic dual gradient generator. A1. Photo of an assembled microfluidic chip on the microscope stage. A2. Layout of a single chip with two devices on a 1 inch x 3 inch glass slide. A3. The design of one dual gradient generator. It contains a microhabitat array (middle) surrounded by 4 side channels, and all of which were patterned in a 1 mm thick agarose gel membrane. A4. The array contains 8 × 8 microhabitats, each has a size of 100 µm x 100 µm x 100 µm, separated by 100 µm from each other. Cells grew in each individual habitat. The four side channels surrounding the microhabitat array provided the dual gradients. Each channel has the width of 400 µm and height of 200 µm. Media containing specific nutrient flow through the source channels and plain medium the sink channels respectively. Two nutrient gradients, one along vertical direction, and the other along horizontal direction, were generated in the microhabitat array region via molecular diffusion through the agarose gel. B1-B4. Characterization of the dual gradient generation using fluorescence dyes. Fluorescein (FITC) solution was introduced to top source channel, rhodamine B solution the right source channel, and plain buffer solution were introduced in the two sink channels at t =0. The fluorescence images of the microhabitat array were taken at t = 90 min with FITC channel (B1) and rhodamine B channel (B3). Contour plots of simulated (lines) and experimental (dots) concentration fields at t = 90 min are shown in B2 for FITC field and B4 for rhodamine B field. Concentration is scaled such that the concentration in source channel is 1 and sink channel 0.

Results and Discussion

Microfluidic setup, dual gradient generation and validation

The microfluidic device was designed such that it provided a dual chemical gradient to the array microhabitats (Fig. 1). The presented work here is an extension of a previous technology developed in our lab where a single gradient array microhabitat device was used for studies of algal cell growth[30]. Briefly, the key component of the device was an 8 × 8 array of microhabitat, each has a size of 100 µm × 100 µm × 100 µm, surrounded by two sets of parallel side channels for nutrient control. Each

control channel was 400 μm wide and 200 μm high (Fig. 1A3-4). We note that the height of each microhabitat was 100 μm while the height of the control channels was 200 μm. The size of the habitat was designed such that the initial cell seeding number was a few cells enabling single cell studies and facilitating cell counting. The height of the channels was chosen to be higher than 100 μm to avoid boundary effect in the vertical direction[33]. By flowing P or N contained medium in the source channels and blank buffer in the sink channels respectively, two concentration gradients of nutrients, N and P, were generated in the array microhabitats via molecular diffusion through agarose gel. The result was that each device has 64 microhabitats, and each has a unique chemical concentrations or N:P concentration ratio. To increase the throughput, two such devices (Fig. 1A2) were patterned side by side onto the 1 mm-thick agarose gel membrane, typically one served as a control and the other provided dual gradients. Cells in both devices were imaged using an automatically controlled microscope stage.

The dual concentration gradients were validated both experimentally and computationally. In the experimental validation, solutions of 100 μM green fluorescence molecules (FITC, 332 Da) and red fluorescence molecules (rhodamine b, 479 Da) in PBS buffer were introduced into the top and right source channels respectively, and blank PBS buffer in the two sink channels at t = 0 (See Fig. 1A3-4). Fluorescence images of the microhabitat array area for FITC (480 nm/520 nm, ex/em, Fig. 1B1) and rhodamine b (562 nm/583 nm, Fig. 1B3) were taken separately at t = 90 min. Here the registered grayscale of the image from the camera is proportional to the concentration of the fluorescence solution[34]. A parallel computation of the nutrient concentration gradients in the array microhabitat was carried out using Fick's second law and constant concentration boundary conditions (For details, please see Supplementary Information). Experimental concentration fields were scaled properly to facilitate a comparison with numerical computation result, such that concentration is 1 in source channels and 0 in sink channels. The scaled experimental concentration field (dots) is plotted against the calculated concentration field (lines) as shown in Fig. 1B2, B4. The experimental concentration field agreed well with that computed numerically, validating the microfluidic device's ability to generate a well-defined dual gradient.

Agarose gel was chosen as the base material for the device, since it allowed the diffusion of molecules[34] such as ammonium and phosphate for gradient generation, but still able to contain cells within each habitat. This differed from PDMS based gradient generator device where convective flow was introduced for gradient generation[23]. In the later case, cells were free to move between habitats, which can complicate the cell growth analysis. For diffusion based gradient generator, a key parameter was the distance between the sink and source channels, since it determined how long it would take for the gradient to be established. While the exact relation can be

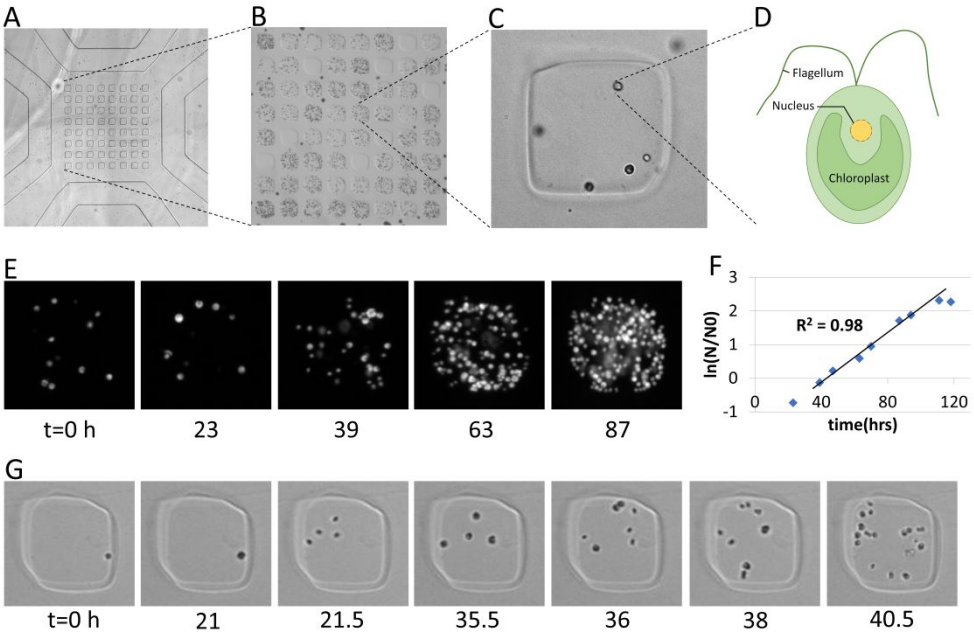

Figure 2. Microalgal cell growth in the microhabitat array. A. A bright field image of the device under microscope. This image was stitched together using four images each taken with a 10x objective. The size of the image is 3.2 mm x 3.2 mm. B. A bright field image of cells in the 8 × 8 array habitats taken using a 4x objective. The size of the image is 1473 μm x 1498 μm. C. A bright field image taken using a 40x objective of cells swimming in one habitat of 100 μm x 100 μm x 100 μm in size. D. Illustration of a photosynthetic eukaryote *C. reinhardtii* cell. The two flagella are responsible for cell motility. E. Fluorescence images of cells growing in one habitat starting t=0 to t=87 hours at about one day time interval. The habitat in each image is 100 μm x 100 μm. F. Growth curve of the cells growing in the habitat shown in E. The cell number N is measured using the fluorescence from each habitat. Dotted lines are experiments, and solid line is a fit to a linear function. The fitted slope (growth rate) was 0.89 ± 0.07 day^{-1}, with R-square value of 0.98. G. Multiple fission of a single *C. reinhardtii* cell in a habitat revealed by a time series bright field images. The habitat in each image is 100 μm x 100 μm. Starting from one single cell at t=0, the four 1st generation daughter cells appeared at 21.5 hours. The 2nd generation cells started to appear at 36 hours, and the division of all four 1st generation cells was completed at 40.5 hours.

computed using Comsol, a simple estimate showed that $x \sim \sqrt{2Dt}$, where x is the distance between sink and souce channels, D is the diffusion coefficient of the interested chemical species, t is the time of gradient establishment[35]. In our device, we chose $x = 2\ mm$ to accommodate 8 microhabitats in a row, with a measured gradient establishment time of ~ 70 minutes (See Fig. S2) which was consistent with the estimate using the equation above.

Growth of *Chlamydomonas reinhardtii* in microhabitat array

Using the array microhabitat device, we first studied the growth of *C. reinhardtii* cells under nutrient-rich conditions. Cells seeded in the microhabitats were shown in Fig. 2A-C. *C. reinhardtii* is a photosynthetic and highly motile eukaryotic green alga with a pair of flagella in the front (Fig. D). Movie S1 showed that cells swam freely within the confinement of each microhabitat. We note that *C. reinhardtii* cells were seeded into the device using a cell-suspension prepared in MM/0.1TAP before the device was assembled. We define t =0, the time when MM/0.1TAP was introduced into the side channels, and the growth of *C. reinhardtii* cells were imaged typically at a 4-hour time interval for about 5 days. Cell growth over a period of 87 hours was clearly seen in Fig. 2E. Using the fluorescence signal in Fig. 2E, we computed total fluorescence from each habitat, and used that as a measure for cell numbers. The resulted growth curve was shown in Fig. 2F. The specific growth rate, λ, was calculated using the exponential growth model $N = N_0 \cdot exp(\lambda t)$, in which N is the total number of cells, N_0 is the initial cell number, and λ is the growth rate.

The advantage of an integrated microfluidic platform with automatic microscope imaging was that it allowed us to follow both fast and slow time events. Here, multiple fission of *C. reinhardtii* cells occurred at a fast time scale, which was captured by the bright field time series imaging with a 30 min interval. Multiple fission is a reproductive pattern unique to algal cells as compared to binary fission in most eukaryotic cells[36]. Multiple fission cell cycles are characterized by a prolonged growth phase when the mother cell's volume experiences a more than two-fold increase, followed by rapid divisions to 4, 8, 16, 32, or even 64 daughter cells[37]. In our microhabitat device, both binary fission and multiple fission of *C. reinhardtii* were observed. Out of the 150 cells observed, majority of the cells (68%) underwent multiple fission to 8 daughter cells, 28% of cells underwent division to 4 daughter cells (Shown in Fig. 2G), and 4% binary fission. Cell cycle time of division to 2, 4, and 8 daughter cells were recorded to be 22.8±1.3, 19.9±5.1, 26.9±3.8 hours respectively. More accurate measurement can be obtained by faster imaging rate. These results showed that the microfluidic platform coupled with automatic imaging provided a unique opportunity for quantitative cell cycle studies of *C. reinhardtii* cell cycles. Various information can be obtained using this platform including mother and daughter cell sizes, cell cycle phase time, and cell cycle regulation protein network [38].

Cell growth under single nutrient gradient

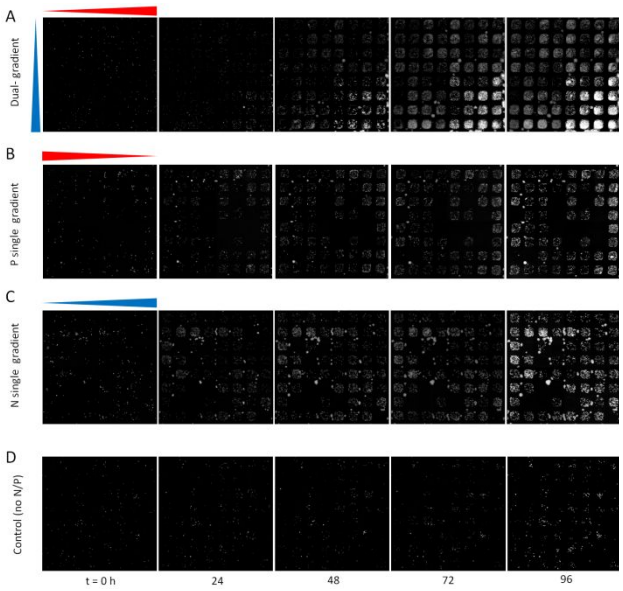

Figure 3. Fluorescence images of cells growing under various nutrient condition. **A.** A time series images of the cells in array microhabitats under dual gradients. P gradient was along horizontal direction and N in vertical direction. **B.** Time series of images under P gradient only. C. Time series of images under N gradient only. D. Time series images under control with plain media in all side channels. For P gradient, 50mM of P solution flows in source channel and plain media flows through sink channel. For N gradient, media with 50mM N flows through source channel and plain media flows through sink channel. For control device, no P or N solution was used, and all side channels were plugged.

Growth of co-limited *C. reinhardtii* cells were studied using single P or N gradient within the microhabitat device (Fig. 3). Two replicates were done for the single P and N gradient respectively, and image of one set was shown in Fig. 3. A single P gradient was created by flowing medium with 50 μM P and no N in the source channel and blank medium with no N/P in the sink channel respectively. The single N gradient was created in a similar way using 50 μM N and no P medium in the source channel and blank medium in the sink channel. The unused two channels were plugged during single gradient experiments. When the device was set up in this way as a single gradient generator, each column of 8 habitats were at the same concentration, with 8 concentrations across the two perfused side channels. Single gradient characterization is shown in Supplementary Information.

The cell growth under single gradients was monitored for 5 days and the fluorescence images of microhabitats were shown in Fig. 3B for single P gradient and Fig. 3C for single N gradient. Combining data from two replicated experiments, mean growth rates of cells in each column were plotted against the nutrient concentration at the middle of the habitat column as shown in Fig. 4A. For each nutrient concentration, data from up to 16 microhabitats were used in the calculation of the mean growth rate and standard error of the mean (SEM). We note that the fitted growth rates along with their errors were used for the final computation of the mean growth rate and SEM in Fig. 4A.

No significant response to P or N single gradient was observed. Since the cells were starved on both nutrients in

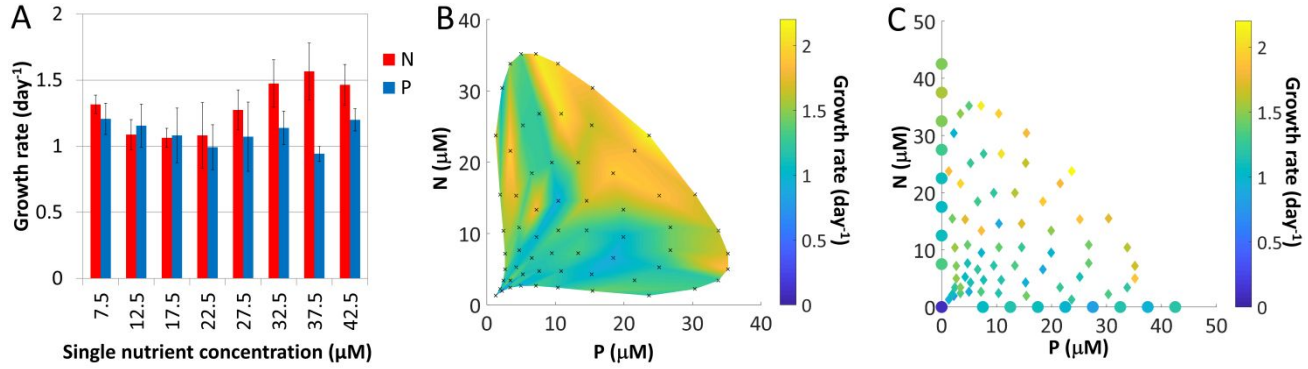

Figure 4. Synergistic roles of P and N on the growth of *C. reinhardtii.* A Growth rate of *C. reinhardtii* under single N (blue) and P (red) gradient. Each data point was calculated using up to 16 data points from two replicated experiments, and error bars represents standard error of the mean (SEM). B. Surface plot of growth rate of *C. reinhardtii* under dual-gradient of N and P. Color represents the value of the growth rate. C. The growth rate of *C. reinhardtii* under: control condition, no N or P (dot at the origin), single P gradient (dots on x axis), single N gradient (dots on Y axis), and dual-gradient (all the diamonds). Color is coded for the value of the growth rate.

advance, their growth in the microhabitats was limited by the nutrient in absence. The fact that there was still growth in these cases could be explained by a minimal amount of nutrients stored in the cells. It is known that *C. reinhardtii* cells can store P in polyphosphates, which may have led to a higher amount of P available for reproductive use. This is consistent with the observation that co-limited cells with added N gradient had an overall higher growth rates than those with the added P gradient (see Figure S3).

Cell growth under dual nutrient gradients

Growth of *C. reinhardtii* cells pre-conditioned in P and N co-limited media were studied in the microhabitat subjected to dual P and N gradients (Fig. 3A). Two replicates were done for dual gradient experiment, and time series images of one experiment in 4 days were shown in Fig. 3A. Starting from a uniformly low cell number in the 8 × 8 array of microhabitats, a bright spot emerged at the bottom right corner, where the N and P concentrations are the highest around day 3 and persistent through day 4. .

Growth rates were calculated for each microhabitat in Fig. 3A and were depicted in the surface plot in Fig. 4B, where the color represents the interpolated growth rate of cells using data from each microhabitats. N-limited growth was seen in the N concentration below 5 μM region, where increasing P concentration alone did not significantly impact the growth rate. In contrast, P-limited growth was not observed at low P region in the surface plot, which was consistent with the fact that the cells were able to store some P and that they utilized more N in proportion to P in their growth. We note that Fig. 4B showed results of one experiment. The duplicate experiment showed a similar trend.

One advantage of a surface plot (see Fig. 4B) is that it allows us to extract additional useful information. For example, one can extrapolate information as to how growth rates behave along the axis of P=N, or a fixed P:N ratio. In addition, by fitting the growth rate versus N concentration at a fixed P value to a Monod kinetics model, we can potentially obtain half saturation constant of *C. reinhardtii* to N at different P concentrations. This calculation showed that more closely spaced data points will be needed for obtaining reliable kinetic constants.

The dual gradient growth rates and single gradient growth rates were presented together in Fig. 4C to further demonstrate the synergistic behaviour of cell growth under dual gradients. Here, each diamond/dot represents a condition of N and P concentrations and the color the growth rate. Taken together, cell growth responded more under both P and N gradients in contrast to single gradient case. At a more subtle level, cells responded to N more sensitively in low P region, while not as much to P gradients at low N region, which was consistent with the fact that cells have the ability to store small amount of P.

Conclusions and future perspectives

We have developed a microfluidic dual gradient generator that provides a well-defined chemical gradient field to an array of 8 × 8 microhabitats for quantitative studies of microalgal growth. This device integrated an array microhabitat and dual gradient format for achieving a high throughput way of examining roles of multiple environmental cues in microalgal growth. Using this device, we investigated the effects of N and P on the growth of *C. reinhardtii*, and found that N and P synergistically promoted the growth of co-limited *C. reinhardtii* cells. Interestingly, no significant response was observed when subjected to single P or N gradient.

While we focused on monitoring the growth of microalgae in this paper, other information can also be obtained using this platform. For example, toxin production in response to environmental factors is a major interest in the study of HAB-forming cyanobacteria, such as microcystin-producing *Microcystis aeruginosa*[39-43]. We can engineer fluorescence probes that can detect toxin biosynthesis activities such that toxin production along with growth can be monitored in the array microhabitat device under a controlled chemical gradient field.

The microfluidic platform presented here can potentially be powerful when coupled with field studies. Results from our

studies can be used to instruct the design of field studies and vice versa. Since experiments using our device is significantly faster, the coupling of in vitro and field studies can accelerate the speed of field studies in a significant way. This is especially important for the study of HABs, as the growth of micro-algal cells were influenced by many environmental factors, including N, P, temperature and light intensity. For example, from year-round field measurements in Lake Taihu, total N was found to be high during winter and low during summer. This raised the question of how N and temperature synergistically impact cell growth[44]. This can be easily tested in the microhabitat devices we developed here.

Looking forward, the array microhabitat device can be easily modified to control other biophysical (e. g. temperature and light intensity) and biochemical (e. g. co-culture) environmental conditions. A light gradient can be created taking advantage of the optics of the microscope and/or design a projector-based custom gradient[45, 46]; a temperature gradient could be incorporated on chip utilizing the Peltier effect; and fluid flow can also be achieved by redesigning the patterns of the micro-channels and habitats. By introducing interconnected microhabitats and microbial community, the device can be used to explore roles of environmental factors in the spatial evolution of the microbial community. It is our hope that the microfluidic platform presented here will contribute significantly to a systematic understanding of the roles of multiple environmental parameters in the behaviour of photosynthetic micro-organisms.

Author Contribution

FL and MW created and designed the research project, FL carried out all the experiments and data analysis, all authors participated in the discussion and writing of the manuscript.

Conflict of interest

There are no conflicts to declare.

Acknowledgements

This work is supported by the USDA National Institute of Food and Agriculture, AFRI project [2016-08830], the Academic Venter Fund from the Atkinson Center for a Sustainable Future, and The New York State Hatch fund. This work was performed in part at Cornell NanoScale Facility (CNF), an NNCI member supported by NSF Grant NNCI-1542081. We thank Tom Pennell, CNF Research Support Specialist for assistance with photolithography. FL and MW thank the help of Dr. Nicole D. Wagner for carefully reading the manuscript, and providing comments; Dr. Beum Jun Kim, Prof. Steve Winans and Prof. Hans Paerl for insightful discussions.

Notes and references

1. H. W. Paerl, T. G. Otten and R. Kudela, *Environ Sci Technol*, 2018, **52**, 5519-5529.
2. M. L. Wells, V. L. Trainer, T. J. Smayda, B. S. O. Karlson, C. G. Trick, R. M. Kudela, A. Ishikawa, S. Bernard, A. Wulff', D. M. Anderson and W. P. Cochlan, *Harmful Algae*, 2015, **49**, 68-93.
3. J. Huisman, G. A. Codd, H. W. Paerl, B. W. Ibelings, J. M. H. Verspagen and P. M. Visser, *Nat Rev Microbiol*, 2018, **16**, 471-483.
4. S. B. Watson, C. Miller, G. Arhonditsis, G. L. Boyer, W. Carmichael, M. N. Charlton, R. Confesor, D. C. Depew, T. O. Hook, S. A. Ludsin, G. Matisoff, S. P. McElmurry, M. W. Murray, R. P. Richards, Y. R. Rao, M. M. Steffen and S. W. Wilhelm, *Harmful Algae*, 2016, **56**, 44-66.
5. H. Xu, H. W. Paerl, G. W. Zhu, B. Q. Qin, N. S. Hall and M. Y. Zhu, *Hydrobiologia*, 2017, **787**, 229-242.
6. J. Leon-Munoz, M. A. Urbina, R. Garreaud and J. L. Iriarte, *Sci Rep-Uk*, 2018, **8**.
7. S. Sliwinska-Wilczewska, A. Cieszynska, M. Konik, J. Maculewicz and A. Latala, *Estuar Coast Shelf S*, 2019, **219**, 139-150.
8. L. Sitoki, R. Kurmayer and E. Rott, *Hydrobiologia*, 2012, **691**, 109-122.
9. R. M. A. Velzeboer, P. D. Baker, J. Rositano, T. Heresztyn, G. A. Codd and S. L. Raggett, *Phycologia*, 2000, **39**, 395-407.
10. M. J. Harke, M. M. Steffen, C. J. Gobler, T. G. Otten, S. W. Wilhelm, S. A. Wood and H. W. Paerl, *Harmful Algae*, 2016, **54**, 4-20.
11. X. C. Li, T. W. Dreher and R. H. Li, *Harmful Algae*, 2016, **54**, 54-68.
12. A. Omidi, M. Esterhuizen-Londt and S. Pflugmacher, *Toxin Rev*, 2018, **37**, 87-105.
13. H. W. Paerl, J. T. Scott, M. J. McCarthy, S. E. Newell, W. S. Gardner, K. E. Havens, D. K. Hoffman, S. W. Wilhelm and W. A. Wurtsbaugh, *Environmental Science & Technology*, 2016, **50**, 10805-10813.
14. D. W. Schindler, *P Roy Soc B-Biol Sci*, 2012, **279**, 4322-4333.
15. M. Z. Liu, J. R. Ma, L. Kang, Y. Y. Wei, Q. He, X. B. Hu and H. Li, *Sci Total Environ*, 2019, **670**, 613-622.
16. T. W. Davis, D. L. Berry, G. L. Boyer and C. J. Gobler, *Harmful Algae*, 2009, **8**, 715-725.
17. M. A. Lezcano, A. Quesada and R. El-Shehawy, *Harmful Algae*, 2018, **71**, 19-28.
18. J. D. Chaffin, T. W. Davis, D. J. Smith, M. M. Baer and G. J. Dick, *Harmful Algae*, 2018, **73**, 84-97.
19. Y. M. Liu, L. Li and R. B. Jia, *Procedia Environ Sci*, 2011, **10**, 2134-2140.
20. G. T. Peng, R. M. Martin, S. P. Dearth, X. C. Sun, G. L. Boyer, S. R. Campagna, S. J. Lin and S. W. Wilhelm, *Environmental Science & Technology*, 2018, **52**, 4127-4136.
21. D. B. Weibel, W. R. DiLuzio and G. M. Whitesides, *Nat Rev Microbiol*, 2007, **5**, 209-218., and references there in.
22. Y. Kalinin, S. Neumann, V. Sourjik and M. M. Wu, *J Bacteriol*, 2010, **192**, 1796-1800.
23. Q. C. Zhang, G. Lambert, D. Liao, H. Kim, K. Robin, C. K. Tung, N. Pourmand and R. H. Austin, *Science*, 2011, **333**, 1764-1767.
24. B. J. Kim and M. M. Wu, *Ann Biomed Eng*, 2012, **40**, 1316-1327., and references therein.
25. X. J. Liu, S. W. Hu, B. Y. Xu, G. Zhao, X. Li, F. W. Xie, J. J. Xu and H. Y. Chen, *Talanta*, 2018, **182**, 202-209.

26. B. Nguyen, P. J. Graham, C. M. Rochman and D. Sinton, *Adv Sci*, 2018, **5**.
27. P. J. Graham, J. Riordon and D. Sinton, *Lab Chip*, 2015, **15**, 3116-3124.
28. Z. Xu, Y. J. Wang, Y. C. Chen, M. H. Spalding and L. Dong, *Biomicrofluidics*, 2017, **11**.
29. C. C. Yang, R. C. Wen, C. R. Shen and D. J. Yao, *Micromachines-Basel*, 2015, **6**, 1755-1767.
30. B. J. Kim, L. V. Richter, N. Hatter, C. K. Tung, B. A. Ahner and M. M. Wu, *Lab Chip*, 2015, **15**, 3687-3694.
31. R. K. Togasaki, K. Brunke, M. Kitayama and O. M. Griffith, in *Progress in Photosynthesis Research: Volume 3 Proceedings of the VIIth International Congress on Photosynthesis Providence, Rhode Island, USA, August 10–15, 1986*, ed. J. Biggins, Springer Netherlands, Dordrecht, 1987, DOI: 10.1007/978-94-017-0516-5_106, pp. 499-502.
32. S. H. Hutner, *J Bacteriol*, 1946, **52**, 213-221.
33. U. Haessler, M. Pisano, M. M. Wu and M. A. Swartz, *Proceedings of the National Academy of Sciences of the United States of America*, 2011, **108**, 5614-5619.
34. S.-Y. Cheng, S. Heilman, M. Wasserman, S. Archer, M. L. Shuler and M. Wu, *Lab Chip*, 2007, **7**, 763-769.
35. H. C. Berg, *Random walks in biology*, Princeton University Press, Princeton, N.J., Expanded edn., 1993.
36. M. A. Borowitzka, J. Beardall, J. A. Raven and SpringerLink (Online service), *The Physiology of Microalgae*, 1st edn.
37. F. R. Cross and J. G. Umen, *Plant J*, 2015, **82**, 370-392.
38. J. G. Umen, *Curr Opin Plant Biol*, 2018, **46**, 96-103.
39. G. M. de la Escalera, C. Kruk, A. M. Segura, L. Nogueira, I. Alcantara and C. Piccini, *Harmful Algae*, 2017, **62**, 73-83.
40. M. Kaebernick, B. A. Neilan, T. Borner and E. Dittmann, *Appl Environ Microb*, 2000, **66**, 3387-3392.
41. J. S. M. Pimentel and A. Giani, *Appl Environ Microb*, 2014, **80**, 5836-5843.
42. A. Srivastava, S. R. Ko, C. Y. Ahn, H. M. Oh, A. K. Ravi and R. K. Asthana, *Biomed Res Int*, 2016, DOI: Artn 598598710.1155/2016/5985987.
43. X. Wang, P. F. Wang, C. Wang, B. Hu, L. X. Ren and Y. Y. Yang, *Ecotox Environ Safe*, 2018, **148**, 942-952.
44. C. M. Zhu, J. Y. Zhang, R. Guan, L. Hale, N. Chen, M. Li, Z. H. Lu, Q. Y. Ge, Y. F. Yang, J. Z. Zhou and T. Chen, *Sci Total Environ*, 2019, **688**, 867-879.
45. G. Frangipane, D. Dell'Arciprete, S. Petracchini, C. Maggi, F. Saglimbeni, S. Bianchi, G. Vizsnyiczai, M. L. Bernardini and R. Di Leonardo, *Elife*, 2018, **7**.
46. A. T. Lam, K. G. Samuel-Gama, J. Griffin, M. Loeun, L. C. Gerber, Z. Hossain, N. J. Cira, S. A. Lee and I. H. Riedel-Kruse, *Lab Chip*, 2017, **17**, 1442-1451.

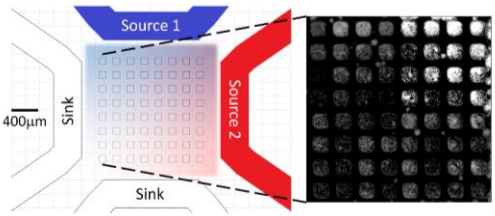

Using an array microhabitat device, we generated dual gradients of critical nutrients, and showed their synergistic effect on microalgal growth.